THE JOURNAL OF BIOLOGICAL CHEMISTRY
Vol. 273, No. 52, Issue of December 25, pp. 35095–35101, 1998
Printed in U.S.A.

Coexpression of the *KCNA3B* Gene Product with Kv1.5 Leads to a Novel A-type Potassium Channel*

(Received for publication, August 28, 1998)

Thorsten Leicher, Robert Bähring, Dirk Isbrandt, and Olaf Pongs‡

From the Institut für Neurale Signalverarbeitung, Zentrum für Molekulare Neurobiologie Hamburg, Martinistraße 52, 20246 Hamburg, Germany

***Shaker*-related voltage-gated potassium (Kv) channels may be heterooligomers consisting of membrane-integral α-subunits associated with auxiliary cytoplasmic β-subunits. In this study we have cloned the human Kvβ3.1 subunit and the corresponding *KCNA3B* gene. Identification of sequence-tagged sites in the gene mapped *KCNA3B* to band p13.1 of human chromosome 17. Comparison of the *KCNA1B*, *KCNA2B*, and *KCNA3B* gene structures showed that the three Kvβ genes have very disparate lengths varying from ≥350 kb (*KCNA1B*) to ~7 kb (*KCNA3B*). Yet, the exon patterns of the three genes, which code for the seven known mammalian Kvβ subunits, are very similar. The Kvβ1 and Kvβ2 splice variants are generated by alternative use of 5′-exons. Mouse Kvβ4, a potential splice variant of Kvβ3, is a read-through product where the open reading frame starts within the sequence intervening between Kvβ3 exons 7 and 8. The human *KCNA3B* sequence does not contain a mouse Kvβ4-like open reading frame. Human Kvβ3 mRNA is specifically expressed in the brain, where it is predominantly detected in the cerebellum. The heterologous coexpression of human Kv1.5 and Kvβ3.1 subunits in Chinese hamster ovary cells yielded a novel Kv channel mediating very fast inactivating (A-type) outward currents upon depolarization. Thus, the expression of Kvβ3.1 subunits potentially extends the possibilities to express diverse A-type Kv channels in the human brain.**

Voltage-gated potassium (Kv) channel diversity has probably evolved to match the various roles of Kv[1] channels in the regulation and control of the electrical potential across the plasma membrane of excitable and nonexcitable cells (1). Different mechanisms have been discovered in recent years that may contribute to the molecular diversity of Kv channels (2–5). Some of the diversity may arise from the multiplicity of genes encoding distinct Kv channel subunits (2, 3). Another means for generating Kv channel diversity is based on the oligomeric structure of Kv channels, which are assembled from different subunits (4). Kvα subunits are integral membrane proteins, assembled as tetramers to form functional Kv channels (5). Assembly of Kvα subunits as homo- as well as heterotetramers may contribute to the expression of diverse Kv channels in the mammalian nervous system (6–8). Kvα may also coassemble with Kvβ subunits, which are auxiliary proteins and associate with distinct cytoplasmic domains of Kvα subunits (9, 10). Most likely, native Shaker-related Kv channels represent heterooligomeric complexes of Kvα and Kvβ subunits in a 1:1 molar ratio (11). While the known Kvβ1 and Kvβ2 subunits have been shown to associate specifically with Shaker-related Kv1α subunits (10), the *Drosophila* Kvβ subunit Hyperkinetic (Hk) appears to associate with Shaker channels and also with EAG and ERG channels (12, 13).

In addition to the *Drosophila* Hk protein, various mammalian Kvβ subunits have been cloned, and studies in heterologous expression systems have shown that the Kvβ subunits may increase the plasma membrane expression (14, 15) and modulate the gating behavior of Kv channels (16–25). Most remarkably, heterologous coexpression of Kvβ1.1 from rat (16, 26) and human brain (23) confers rapid inactivation on otherwise noninactivating delayed rectifier channels. It could be shown that Kvβ1.1 contains a distinct N-terminal sequence similar to the N-terminal structures of rapidly inactivating (A-type) Shaker channels (16). This structure functions as an inactivating "ball" domain (27), which, upon depolarization, can occlude the channel pore by binding to a receptor near or at the cytoplasmic side of the pore (28). It has been shown that several splice variants of Kvβ1 (Kvβ1.1, Kvβ1.2, and Kvβ1.3) exist, which have variant N-terminal sequences and accordingly variant inactivating domains (18–23) and yet have similar functional properties.

We previously cloned another Kvβ subunit from rat brain, Kvβ3 (17). It also contains an N-terminal inactivating domain that is similar in structure and function to the ones found in some Shaker Kvα and in Kvβ1 subunits (17, 26). Coexpression of rat Kvβ3 in *Xenopus* oocytes conferred rapid inactivation on Kv1.4Δ1–110 channels but not on other Kv1α channels (17). In this study, we present structural and functional properties of the human *KCNA3B* gene and the encoded Kvβ3.1 subunit, respectively. In contrast to *Xenopus* oocytes, coexpression of Kvβ3.1 from human brain in Chinese hamster ovary (CHO) cells conferred rapid inactivation on human Kv1.5 channels. Apparently, Kvβ3.1 and Kv1.5 assemble to a novel type of heteromultimeric A-type channel, which inactivates completely and significantly faster than previously *in vitro* expressed A-type Kv channels. Thus, Kvβ3.1 subunits potentially extend the possibilities to express diverse A-type Kv channels in the human brain.

EXPERIMENTAL PROCEDURES

Isolation and Analysis of hKvβ3.1 cDNA

A human brain cDNA library in λgt10 (CLONTECH) was hybridized in 5× SET (75 mM NaCl, 0.5 mM EDTA, 15 mM, Tris-HCl, pH 7.4), 1% SDS, 50% formamide, 5× Denhardt′s solution, and 0.1 mg/ml dena-

* This work was supported by grants of the Deutsche Forschungsgemeinschaft and Fonds der Chemischen Industrie. The costs of publication of this article were defrayed in part by the payment of page charges. This article must therefore be hereby marked "*advertisement*" in accordance with 18 U.S.C. Section 1734 solely to indicate this fact.

‡ To whom correspondence should be addressed: Institut für Neurale Signalverarbeitung, Zentrum für Molekulare Neurobiologie, Martinistraße 52, 20246 Hamburg, Germany. Tel.: 49 40 4717 5081; Fax: 49 40 4717 5102; E-mail: pointuri@uke.uni-hamburg.de.

[1] The abbreviations used are: Kv, voltage-gated potassium; hKv, human Kv; mKv, murine Kv; CHO, Chinese hamster ovary; ORF, open reading frame; STS, sequence-tagged sites; PCR, polymerase chain reaction; bp, base pair(s); kb, kilobase pair(s).

tured herring testis DNA at 42 °C with a rat Kvβ3.1 cDNA probe (nucleotides 658–1198; accession no. X76723) labeled by random priming (29) with [α-^{32}P]dCTP. Filters were washed in 1× SET, 0.1% SDS at 65 °C. Exposure to x-ray films (Kodak BioMax MS) was overnight with an amplifying screen (Cronex Hi$^+$, DuPont), at −70 °C. Eight positive phages were isolated with hKvβ3 cDNA inserts varying in length between 0.9 and 1.9 kb. cDNA inserts were cloned into the *Eco*RI site of pBluescript KS$^-$ (Stratagene). Both strands were sequenced using the dideoxy chain termination method (30) and a T7 sequencing kit from Amersham Pharmacia Biotech. Genetics Computer Group Inc. (GCG, Madison, WI) software was used for sequence analysis. The sequence of the open reading frame (ORF) has been submitted to the National Center for Biotechnology Information (NCBI) data bank (accession no. AF016411).

Isolation and Sequence Analysis of Genomic DNA

KCNA2B Gene—hKvβ2-specific probes were generated using specific PCR fragments of the coding and noncoding region. The *KCNA2B*-specific primer sequences are available on request (31). A human genomic library in λEMBL3 SP6/T7 (CLONTECH) was hybridized with [α-^{32}P]dCTP-labeled hKvβ2 probes as described (see above and Ref. 23). Twenty-five positive phages were isolated with *KCNA2B* DNA inserts varying in length between 14 and 20 kb. Restriction site mapping of phage inserts was carried out using standard protocols. Subcloned restriction fragments containing exon sequences were sequenced for genomic and cDNA sequence alignments. The 5′-termini of phage inserts 3, 18, 21, 24, 26, 62, 69, and the 3′-termini of phage inserts 18, 21, 23, 24, 62, 64, and 69 were used as probes to construct the contiguous *KCNA2B* map shown in Fig. 1. A detailed map is available on request (31). Genomic and cDNA sequence alignments were done with GCG software.

KCNA3B Gene—The λEMBL3 SP6/T7 genomic DNA library was hybridized with a [α-^{32}P]dCTP-labeled hKvβ3 probe (nucleotides 1–1215). Hybridization conditions were as above. One positive phage was isolated containing the complete *KCNA3B* gene. The insert DNA (11.85 kb) was subcloned and completely sequenced using the dideoxy chain termination method (31). The sequence was analyzed employing GCG software and the electronic PCR program of the NCBI data bank.[2]

Chromosomal Localization

DNA panels from human/rodent hybrid somatic cell lines were purchased from BIOS Laboratories (Scotlab GmbH, Wiesloch, Germany). PCR and chromosomal localization studies were performed using primers B3–107 (ACCCAAAGTGAGGGGATATG) and B3–208 (CTGCTTTTACCCTCCATAGG). The primers amplify a 620-bp product from human genomic DNA, corresponding to nucleotides 8327–8947 of the *KCNA3B* gene. The PCRs were carried out with 100 ng of genomic DNA as template, 20 pM of each primer and 1.5 units of *Taq* polymerase (Life Technologies, Inc.) in buffer containing 10 mM Tris-HCl (pH 8.3), an 80 μM concentration of each dNTP, and 1 mM $MgCl_2$. Amplification was carried out for 35 cycles (each cycle consisting of 94 °C for 1 min; 60 °C for 30 s; 72 °C for 30 s).

Northern Blot Analysis

Northern blots of human brain poly(A$^+$) mRNA were obtained from CLONTECH. The blots were hybridized according to the manufacturer′s protocol with a [α-^{32}P]dCTP-labeled hKvβ3.1 cDNA probe (nucleotides 1–550 or 912–1162). Control hybridizations were done with an actin probe supplied by the manufacturer. After three washes with 0.5× SET, 0.1% SDS at 65 °C, membranes were autoradiographed. Exposure to x-ray films (Kodak BioMax MS) was for 72 h with an amplifying screen (Cronex Hi$^+$, DuPont) at −70 °C.

Channel Expression and Functional Characterization

Both hKvα1.5 and hKvβ3.1 cDNAs were cloned into the eucaryotic expression vector pcDNA3 (Invitrogen). Recombinant Kvα1.5 cDNA (10 ng/μl) alone or together with Kvβ3.1 cDNA (200 ng/μl) was microinjected into CHO cells with green fluorescent protein cDNA (5 ng/μl) as a reporter gene to allow the identification of injected cells during electrophysiological experiments. A 20-fold excess of β-subunit cDNA was used to favor high expression, which should allow maximal αβ interaction. Currents activated by depolarizing voltage pulses in the outside-out patch configuration were obtained 12 h after DNA injection. Patch pipettes were pulled from borosilicate capillaries using a DMZ puller (Zeitz, Augsburg, Germany) and had bath resistances between 3 and 4 MΩ when filled with an intracellular solution containing 115 mM KCl, 1 mM $CaCl_2$, 1 mM $MgCl_2$, 11 mM EGTA, 10 mM HEPES, 2 mM Na_2ATP, and 2 mM glutathione, pH 7.2, KOH. The bath solution contained 135 mM NaCl, 5 mM KCl, 2 mM $CaCl_2$, 2 mM $MgCl_2$, 5 mM HEPES, 10 mM glucose, 20 mM sucrose, pH 7.4, NaOH. Currents were recorded with an EPC9 patch clamp amplifier (HEKA Elektronik, Landbrecht, Germany), and the program package PULSE + PULSEFIT (HEKA Elektronik) was used for data acquisition and analysis. Activation and inactivation kinetics were fitted simultaneously with a Hodgkin-Huxley-related formalism (PULSEFIT) as described previously (32). Voltage-dependent processes were fitted with Boltzmann functions of the form $G/G_{max} = (1/1 + \exp((V_m - V_{½})/k))^n$. For a first power Boltzmann function ($n = 1$), which was used to fit steady-state inactivation, $V_{½}$ is the potential of half-maximal inactivation. For a fourth power Boltzmann function ($n = 4$), which was used to fit channel activation, $V_{½}$ is the potential at which each of the four subunits is activated half of the time. The latter $V_{½}$ value yielded an estimate of the activation threshold ($0.5^4 = 6.25\%$ of the maximal activation). The steepness of voltage dependences is described by the slope factor k. Data are given as mean ± S.E. All experiments were performed at room temperature.

RESULTS

Cloning of Human Voltage-gated Potassium Channel Kvβ3.1 cDNA—To isolate human Kvβ3.1 cDNA, we prepared a ^{32}P-labeled rat Kvβ3 cDNA probe for screening a human brain cDNA library (see "Experimental Procedures"). Eight phages were isolated, and the inserts were subcloned and sequenced. One insert of 1857 bp contained the complete Kvβ3.1 ORF. The derived human Kvβ3.1 protein sequence has a length of 404 amino acids (Fig. 1).

The hKvβ3.1 sequence shares 92.3% identity with the previously published rat Kvβ3 protein sequence (17). This contrasts with an identity of 74.6% to the human Kvβ2.1 and 72.4% to the human Kvβ1.1 protein sequence, respectively. Alignment of hKvβ1.1, hKvβ2.1, and hKvβ3.1 sequences showed that the amino termini are highly divergent (Fig. 1). The remaining carboxyl-terminal Kvβ sequences are conserved and share a sequence identity of 85%. Accordingly, several consensus sequences for the possible phosphorylation by protein kinases have been conserved between the different hKvβ protein sequences (Fig. 1). Remarkably, only one of the 10 consensus sites is a protein kinase A phosphorylation site.

Similar Exon/Intron Structure for Kvβ1, Kvβ2, and Kvβ3 Genes—Previously, we have cloned the human Kvβ1 (*KCNA1B*) gene (23). A comparison of the genomic DNA sequence with human Kvβ1 cDNA showed that the *KCNA1B* gene has an exceptionally large size of >380 kb. The Kvβ1 ORFs are composed of 14 exons, and the first exon(s) (1.1, 1.2, and 1.3 in Fig. 2*A*) encode the alternative Kvβ1 amino termini. Now, we have cloned the human Kvβ2 (*KCNA2B*) and Kvβ3 (*KCNA3B*) genes. A ^{32}P-labeled human hKvβ2.1 cDNA (21) was used to probe a human genomic λ-phage library. In order to construct a physical map of 91-kb DNA containing the *KCNA2B* gene, 25 positive partially overlapping phages were isolated (Fig. 2*B*). A comparison of the genomic sequence with the hKvβ2.1 cDNA revealed 15 exons (spread out over ~70-kb DNA. The last exon of the *KCNA2B* ORF contained an additional 1800 bp of 3′-untranslated sequence. The size of the intervening introns varied between 236 bp and 33 kb. All exon/intron borders followed the GT/AG rule (33). In contrast to Kvβ1 amino termini, the corresponding hKvβ2 amino terminus is encoded in two exons (1a and 1b in Fig. 2*A*). Skipping of exon 1b may give rise to the hKvβ2.2 splice variant, which has been discovered recently in human lens epithelium (accession no. AF044253).

To characterize the *KCNA3B* gene we probed a human genomic λ-library with ^{32}P-labeled hKvβ3.1 cDNA. One phage was isolated, containing an 11.8-kb insert. It encoded apparently the complete *KCNA3B* gene (Fig. 2*B*). In comparison, the *KCNA3B* gene is approximately 50 times smaller than the

[2] Available on the World Wide Web at http://www.ncbi.nlm.nih.gov.

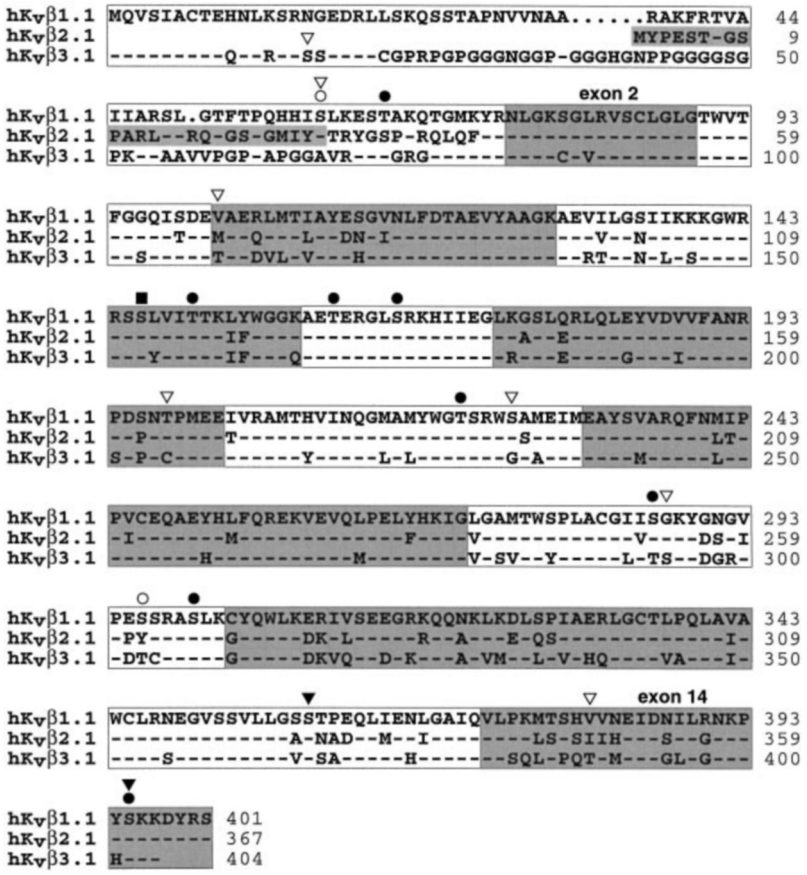

FIG. 1. **Alignment of derived hKvβ1.1, hKvβ2.1, and hKvβ3.1 subunit sequences.** Sequence of hKvβ3.1 was aligned with the ones of hKvβ1.1 (23) and hKvβ2.1 (43) using BEST FIT. Amino acids are given in the standard single-letter codes. *Numbers* on the *right* refer to the last amino acid of the corresponding sequence. *Dots* indicate gaps introduced for optimal sequence alignment. Identical amino acids are indicated by *dashes*. Exons along the derived polypeptide sequences are indicated by *alternatively shaded boxes*. For orientation, exons 2 and 14 have been labeled. Potential phosphorylation sites for protein kinase A (■), for protein kinase C (○) and casein kinase II (▽) have been marked. *Filled symbols* indicate conserved sites found in all three Kvβ subunits.

KCNA1B gene and approximately 10 times smaller than the *KCNA2B* gene. Alignment of the genomic *KCNA3B* DNA and hKvβ3.1 cDNA sequences showed that the *KCNA3B* gene comprised 14 exons (Fig. 1), comparable in size and structure with those of the *KCNA1B* and *KCNA2B* genes (Fig. 2*A*). All exon/intron borders followed the GT/AG rule (33). The last exon contained a 3′-untranslated sequence with two consensus polyadenylation signals (AATAAA) 752 and 760 bp downstream of the ORF stop codon, respectively. The results demonstrate that the different hKvβ genes contain very similar exon patterns (Figs. 1 and 2). Thus, the greatly varying size of the Kvβ genes, ranging from >380 kb (*KCNA1B*) to ~7 kb (*KCNA3B*), is largely due to differences in the sizes of the intervening introns; the *KCNA1B* gene contains some introns of ≥50kb, whereas introns of the *KCNA3B* gene have sizes of ≤1.4 kb (Fig. 2*B*).

KCNA3B Located on Chromosome 17p13.1—The genomic *KCNA3B* sequence information was used to choose a primer pair 5′ and 3′ to exon 8. The primer pair specifically amplified a 620-bp *KCNA3B* DNA fragment in PCRs using human genomic DNA as template but not in PCRs with mouse or hamster genomic DNA as template. In PCRs with a DNA panel of human/mouse/hamster hybrid cell lines, the 620-bp *KCNA3B* DNA fragment was only amplified with template DNA derived from hybrid DNA cell lines containing human chromosome 17 (not shown). A search in the NCBI dbSTS data bank revealed the two identical sequence-tagged sites (STS) SHGC 31899 and dbSTS 38881 (Fig. 2*B*) 50 bp upstream of the first polyadenylation site of the *KCNA3B* sequence. They have been mapped to band p13.1 on the short arm of human chromosome 17. Thus, the *KCNA3B* gene was localized between the microsatellite markers D17S786 and D17S960 (Ref. 34; Fig. 3).

The microsatellite markers are located near the genes for the postsynaptic density protein 95 (34) and retinal guanylate cyclase (35). Mutations in the retinal guanylate cyclase gene cause a form of Leber congenital amaurosis (36) and an autosomally inherited dominant form of progressive cone dystrophy (CORD6; Ref. 37). Two-point analyses in a five-generation Swedish family carrying the CORD5 syndrome demonstrated linkage to the markers D17S786 and D17S960 with maximum logarithmic odds ratio scores of 6.5 and 4.4, respectively (39). Since these markers flanked the *KCNA3B* gene, we analyzed DNA obtained from Swedish families with CORD5-affected members. The results did not reveal mutations in the *KCNA3B* exon sequences. Apparently, CORD5 is not linked to the *KCNA3B* gene.

Tissue-specific Expression of hKvβ3.1 mRNA—The distribution of Kvβ3.1 mRNA in human tissue and in various areas of human brain was investigated in Northern blot analysis. With a Kvβ3.1 cDNA-specific probe, we detected two mRNAs of 2.8 and 4.4 kb in brain but not in heart, lung, liver, kidney, pancreas, placenta, and skeletal muscle (Fig. 4*A*). The exon structure of the *KCNA3B* gene predicts a ~4.4-kb-long transcript. The 2.8-kb transcript may correspond to an as yet undetected Kvβ3 splice variant comparable with mouse Kvβ4 (Ref. 14; see "Discussion").

The expression of hKvβ3.1 mRNA in human brain was analyzed in more detail using Northern blots containing mRNA derived from several brain areas. We obtained a strong hybridization signal for Kvβ3.1 mRNA with poly(A^+) RNA of human cerebellum, weaker signals with the ones of cortex, occipital lobe, frontal lobe, and temporal lobe (Fig. 4*B*). No significant hybridization signals were obtained with poly(A^+) RNA of medulla and spinal cord (Fig. 4*B*) as well as amygdala, caudate nucleus, corpus callosum, hippocampus, hypothalamus, substantia nigra, subthalamic nucleus, and thalamus (data not shown). The results suggest similar mRNA expression patterns

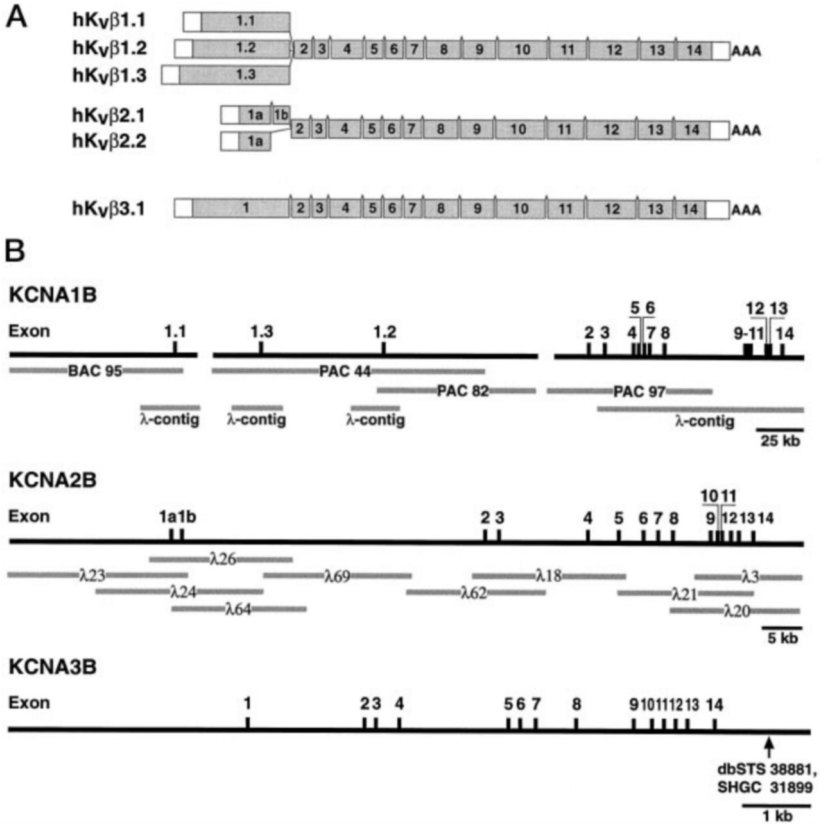

FIG. 2. **Exon/intron structures of *KCNA1B*, *KCNA2B*, and *KCNA3B* genes.** *A*, comparison of the exon compositions of hKvβ1, hKvβ2, and hKvβ3 type subunits. Exons are depicted as *numbered rectangles*. Sizes are approximately to scale except for the first and last exons. Untranslated 5′- and 3′-sequences are not *shaded*. The 5′-borders of exons 1 have not been determined. Alternative 5′-exons for hKvβ1 splice variants are indicated as *1.1*, *1.2*, and *1.3*. hKvβ2 splice variants either contain exons 1a and 1b or only 1a. Exons 14, which contain varying lengths of 3′-untranslated sequences including the signals for polyadenylation (AAA), are not drawn to scale. The hKvβ1 exon pattern has been adopted from Ref. 23. *B*, comparison of physical maps of *KCNA1B*, *KCNA2B*, and *KCNA3B* genes. *Thick horizontal bars* correspond to cloned genomic DNA. *Scale bars* are at the *bottom right*. Part of *KCNA1B* map has been published previously (23). *Gray bars* indicate recombinant DNAs used for constructing a physical map of the *KCNA1B* and *KCNA2B* genes. Genomic *KCNA3B* DNA was contained in one λ phage (not indicated). *BAC*, bacterial artificial chromosome; *PAC*, P1 artificial chromosome; λ-*contig*, contiguous stretch of genomic DNA cloned by overlapping λ-phages; λ, λ-phage followed by clone number. Positions of exons on the physical maps are indicated by *small vertical bars*. The direction of transcription is from *left* to *right*. Exons are numbered as in *A*. Note that *KCNA1B* exon 1.1 may be located either 5′ to exon 1.3 or 3′ to exon 1.2, because the *KCNA1B* map contains two gaps. The *arrow* indicates the location of STS SHGC 31899 and dbSTS 38881 on the *KCNA3B* map.

of Kvβ3.1 in human and rat brain (17) except for thalamic nuclei.

Functional Expression of hKvβ3.1—We have previously shown that hKvβ1.1 subunits confer rapid inactivation to hKv1.5 channels when coexpressed in mammalian tissue culture cells (23). In the present study, we tested a possible interaction between hKv1.5 and hKvβ3.1 subunits. The injection of hKv1.5 cDNA alone in CHO cells led to the expression of channels mediating typical outward currents with fast activation in response to depolarizing voltage pulses (Ref. 40; Fig. 5*A*). Kv1.5-mediated currents inactivated slowly, resulting in 70.9 ± 1.6% (n = 6) of the peak current at the end of a 1-s pulse to +60 mV. Inactivation kinetics were best described by two exponentials with time constants τ_1 = 70.0 ± 14.0 ms (28.1 ± 4.3% of the total decay) and τ_2 = 1.5 ± 0.3 s (n = 5).

When we coexpressed hKvβ3.1 with hKv1.5, rapidly inactivating potassium currents were elicited upon depolarization (Fig. 5*A*). With equimolar injection of Kvα and Kvβ subunit cDNA (10 ng/μl of each), we obtained currents with rapid but largely incomplete decay (data not shown). Apparently, in these experiments the steady-state current component represented a distinct population of noninactivating channels rather than equilibrium conditions of a single rapidly inactivating channel population. The current decay at +60 mV was virtually complete (2.3 ± 0.3% of the peak current at the end of a 1-s pulse) in 25 out of 29 patches when the amount of injected Kvβ cDNA was increased 20-fold (Fig. 5*A*). The inactivation kinetics of hKv1.5 channels in combination with hKvβ3.1 subunits were best described by two exponentials with τ_1 = 5.8 ± 0.4 ms (87.6 ± 2.1% of the total decay) and τ_2 = 32.2 ± 4.2 ms (n = 25). The steady-state inactivation due to the presence of hKvβ3.1 showed a steep voltage dependence with $V_{½}$ = −29.0 ± 1.1 mV and k = 2.7 ± 0.2 mV (n = 5; Fig. 5*B*). The recovery from inactivation measured at −80 mV showed a fast component with τ_1 = 0.8 ± 0.2 s, accounting for 48.9 ± 11.7% of the complete recovery followed by a slower component with τ_2 = 4.6 ± 0.9 s (n = 4; Fig. 5*C*).

Many investigators have described a hyperpolarizing shift in the voltage dependence of channel activation, when Kvα subunits were coexpressed with Kvβ subunits (24–26, 41, 42). We tested the voltage dependence of hKv1.5 channel activation using a pulse protocol with a holding potential of −80 mV and test potentials between −50 and +100 mV. For the expression of hKv1.5 alone, a fourth power Boltzmann-function (see "Experimental Procedures") was fit to the conductance-voltage relationship (Fig. 5*D*; *open circles*) with a $V_{½}$ = −32.3 ± 0.8 mV and a slope factor k = 21.0 ± 0.6 mV (n = 6). The value for $V_{½}$ obtained by Heinemann *et al.* (26) from a similar Boltzmann analysis of Kv1.5 channel activation in *Xenopus* oocytes is slightly more negative, and their slope factor k suggests a steeper voltage dependence of gating. For the coexpression of hKv1.5 and hKvβ3.1 in CHO cells, Boltzmann analysis yielded

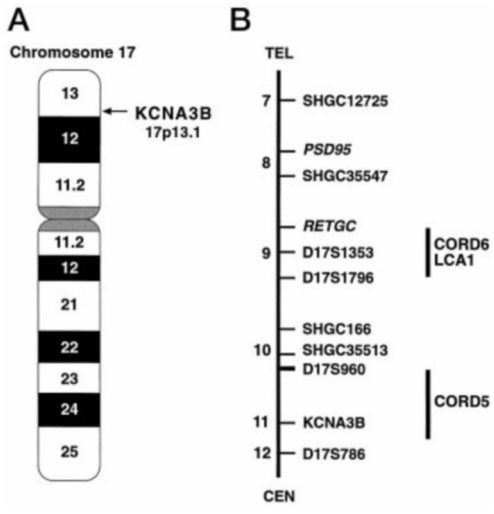

FIG. 3. **Chromosomal localization of *KCNA3B*.** *A*, a somatic hybrid panel screen localized the *KCNA3B* gene to chromosome 17. The presence of STS SHGC 31899 and dbSTS 38881 at the 3′-end of the *KCNA3B* gene refined its chromosomal map position to 17p13.1. *B*, detailed map of the 17p13.1 region with locations of microsatellite markers and the genes for postsynaptic density protein 95 (*PSD95*) (35), retinal guanylate cyclase (*RETGC*) (36), and *KCNA3B*. Linkage of Leber congenital amaurosis type 1 (*LCA1*) (37) and autosomal dominant progressive cone dystrophies (CORD5 and -6) (39, 49) to microsatellite markers is indicated by *bars* on the *right*. *TEL-CEN*, orientation of map from telomer to centromer. The Stanford Human Genome Center bin number assigned for each marker is given on the *left*.

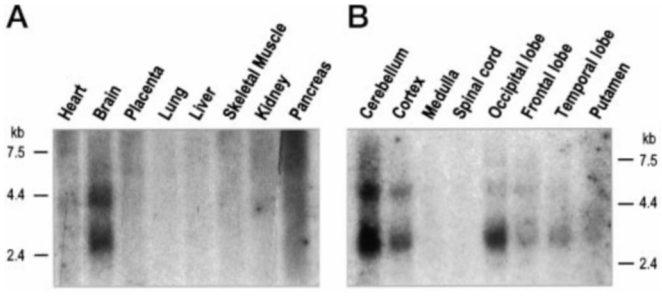

FIG. 4. **Tissue specificity of hKvβ3 mRNA expression.** Commercial Northern blots (CLONTECH) of poly(A^+) mRNA derived from adult human tissues (*A*) and specific human brain areas (*B*), as indicated at the *top* of each *lane*, were hybridized with a α-^{32}P-labeled hKvβ3.1 cDNA probe (nucleotides 1–550). Each *lane* contained 2 μg of poly(A^+) mRNA. Size markers (in kb) are on the *left*. Blots were autoradiographed for 72 h.

$V_{½} = -31.7 \pm 2.5$ mV and a slope factor $k = 28.3 \pm 1.5$ mV ($n = 5$) if conductance voltage plots were derived from the measured peak amplitudes (Fig. 5*D*, *filled triangles*). However, the current peaks may not reliably reflect steady-state channel activation at a given membrane potential, because rapid inactivation occurs already during the activation phase, leading to an underestimation of the maximal activation. Therefore, we used simulated I_{max} values based on a model with no inactivation (Hodgkin-Huxley-related formalism with $h = 4$ and $m = 0$) to create conductance-voltage plots (Fig. 5*D*, *inset* and *filled circles*). The values obtained with Boltzmann analysis were $V_{½} = -31.9 \pm 2.1$ mV and $k = 20.0 \pm 2.3$ mV ($n = 5$), suggesting no significant alteration in the voltage dependence of hKv1.5 channel activation by the presence of hKvβ3.1 subunits ($p = 0.8518$; two-tailed t test).

DISCUSSION

This paper presents a comparative analysis of the structure of human genes encoding Kvβ subunits and the functional expression of a new human Kvβ subunit.

Kvβ Gene Structures—The Kvβ genes map to different chromosomes. *KCNA1B* is located on chromosome 3q25.1 (23), *KCNA2B* on 1p36 (43), and *KCNA3B* on 17p13.1 (this paper). Despite their different chromosomal locations, the *KCNAB* genes have a similar exon/intron pattern. This pattern reflects the conserved structure of Kvβ proteins. They have differing amino termini, varying in length from 26 to 91 amino acids and a highly conserved carboxyl terminus of ~325 amino acids. The variant Kvβ1.1, -1.2, -1.3, and -3.1 amino termini are encoded each in a distinct exon. Thus, the different Kvβ1 subunits are produced by alternative splicing of exons 1. By contrast, the alternative Kvβ2 amino termini may be generated by an exon-skipping mechanism, leaving out exon 1b (Fig. 2*A*). The 5′-terminal exons are spliced to a Kvβ "core" region. It invariably consists of 13 exons that are highly homologous among the three genes. In contrast to the exon pattern, the *KCNA1B*, *KCNA2B*, and *KCNA3B* genes contain intervening sequences, which vary markedly in length. Accordingly, the *KCNA1B* gene is ~50 times larger and the *KCNA2B* gene ~10 times larger than the *KCNA3B* gene. The similarity of the exon/intron patterns, despite the greatly varying sizes of the different genes, suggests that the three human Kvβ genes were derived from an ancestral precursor gene. The data indicate that unlike Kvα subunit genes (44, 45) Kvβ subunit genes are not clustered in the human genome. Most likely, Kvβ subunit diversity has evolved from chromosomal rearrangements rather than from local gene duplications.

Another Kvβ genomic structure has been reported for *Drosophila Hk*. The derived Hk protein sequence of 546 amino acids indicates that this Kvβ subunit is considerably larger than the human Kvβ subunits. Yet, the Hk ORF comprises six instead of 14 exons (12). Due to the lack of detailed sequence information, it is not clear how *Hk* exons relate to hKvβ exons. Nevertheless, the nonconserved exon/intron structures between *Drosophila* and humans suggest that they have arisen in evolution after the separation of vertebrates and invertebrates. Interestingly, the exon/intron structures of *Drosophila Shaker* and human Kvα subunit genes (2, 3) are not similar either, despite the highly conserved protein sequences of Shaker-related Kvα subunits (2).

Kvβ3.1 mRNA Expression—The hKvβ3.1 cDNA probes hybridized to two mRNA species (4.4 and 2.8 kb in length) in the Northern blot experiments. The longer transcript is consistent with our genomic sequence analysis of the *KCNA3B* gene, which predicts a hKvβ3.1 mRNA length of 3868 nucleotides without the poly(A) tail. The shorter transcript may be a cross-hybridizing mRNA species or an alternatively spliced *KCNA3B* transcript. This notion may be supported by a recent report describing a Kvβ4 subunit in mice (14). A comparison of the derived hKvβ3.1 and mouse Kvβ4 protein sequences revealed that both differ in their amino termini, whereas the carboxyl termini consisting of 225 amino acid residues are nearly identical, sharing an identity of 95%. The hKvβ3.1/mKvβ4 sequence identity starts exactly with the first amino acid of *KCNA3B* exon 8. Analysis of the mouse Kvβ3 gene showed that the mouse Kvβ4 amino terminus is encoded in the intron 7 sequence preceding mouse exon 8 (Fig. 6). This indicates that mKvβ4 is translated from a mouse Kvβ3 mRNA variant where intron 7 is not spliced out. The mouse and human intron 7 sequences have a similarity of 70%. However, an *Alu* element is inserted into human intron 7 DNA (Fig. 6). Therefore, the *KCNA3B* cannot code for a Kvβ3 variant that is analogous to mKvβ4.

Rapid Kv Channel Inactivation Conferred by Kvβ3.1—Kvβ1 and Kvβ2 subunits can assemble with Shaker-related Kvα subunits both *in vitro* (9, 10, 16) and *in vivo* (46). This assembly

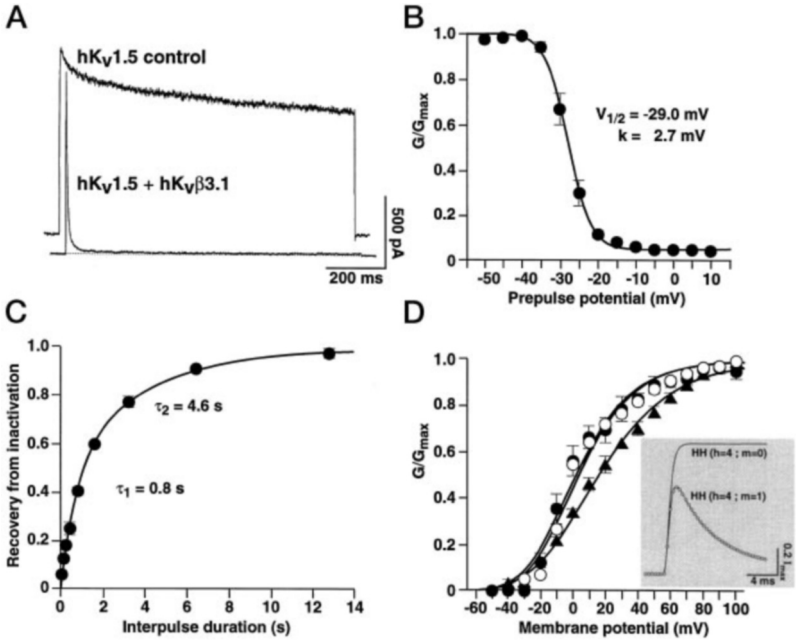

FIG. 5. **Properties of hKvα1.5 channels coexpressed with hKvβ3.1 in CHO cells.** *A*, outward currents during voltage pulses of 1 s to +60 mV from a holding potential of −80 mV recorded in outside-out patches excised from two different CHO cells. One cell was injected with hKvα1.5 cDNA alone (slow and incomplete decay), and in the other cell hKvα1.5 and hKvβ3.1 cDNAs were coinjected (rapid and virtually complete decay). Two current traces with equal peak amplitudes were chosen for illustrative purposes. *B*, voltage dependence of steady-state inactivation. Data points represent current amplitudes normalized to the maximal peak obtained at +60 mV following a prepulse of 500-ms duration to potentials between −50 and +10 mV in 5-mV steps from a holding potential of −80 mV. The curve fitted to the data points represents a first power Boltzmann function. Mean values for $V_{½}$ and k as indicated. *C*, recovery from inactivation measured with a set of twin pulses to +60 mV separated by intervals of different length at −80 mV. The *line* fitted to the data points represents a double-exponential function with the mean values for τ_1 and τ_2 as indicated. *D*, voltage-dependent activation of hKv1.5 channels in the absence (*open circles*) and presence of hKvβ3.1 (*filled triangles*). Conductance-voltage plots were obtained from the peak amplitudes measured during 200-ms pulses to potentials between −50 and +100 mV in 10-mV increments from a holding potential of −80 mV. Conductance values were normalized to the value obtained at +100 mV. *Open circles* represent conductance values obtained by using a calculated I_{max} not accounting for inactivation. The *inset* illustrates fitting of a Hodgkin-Huxley-related formalism to a recorded A-type current trace (only 25% of acquired data points are shown for clarity). I_{max} was with the obtained parameters for activation calculated by setting $m = 0$. This eliminates inactivation from the model. Curves fitted to the conductance-voltage plots represent fourth power Boltzmann-functions. Mean values for the respective parameters were as follows: $V_{½} = -32.3$ mV and $k = 21.0$ (hKv1.5); $V_{½} = -31.7$ mV and $k = 28.3$ (hKv1.5 + hKvβ3.1); $V_{½} = -31.9$ mV and $k = 20.0$ (from simulated I_{max} values). Note that no apparent shift in activation threshold was observed irrespective of the method of analysis.

may enhance the surface expression of Kv1α subunits, leading to an increased number of Kv channels in the plasma membrane (15). In addition, Kvβ1 but not Kvβ2 subunits may affect the inactivating properties of Kv1α subunits (18–20, 47). Kvβ1.1 contains an N-terminal inactivating domain, which confers rapid N-type inactivation to otherwise noninactivating channels of the Kv1 family (16). The Kvβ1.1 N-terminal inactivating domain is similar in structure and function to the ones of Shaker channels (16). They inactivate the channel by binding to a receptor at or near the inner pore entrance (28), resembling a tethered ball and chain type mechanism (27). The Kvβ3.1 amino terminus also has the characteristic features of N-terminal inactivating domains (17). Coexpression of rat Kvβ3 in *Xenopus* oocytes imposed rapid inactivation on Kv1.4Δ1–110 channels, and the sensitivity of this inactivation to intracellular redox potential and its kinetics were comparable with the inactivation conferred on Kv1.4Δ1–110 channels by Kvβ1.1 (17). However, it was not possible to detect in the *Xenopus* oocyte expression system functional assemblies of Kvβ3 with Kv1.1 or Kv1.5 channels (26). In the present study, we show that hKvβ3.1 subunits confer rapid inactivation to hKv1.5 channels upon coexpression in CHO cells. From a kinetic point of view, the Kv1.5/Kvβ3.1-mediated A-type channel shows the fastest inactivation of all cloned Kv channels that have been heterologously expressed so far. The time course and the completeness of inactivation as well as the parameters for both steady-state inactivation and recovery from inactivation obtained in our experiments are in excellent agreement with

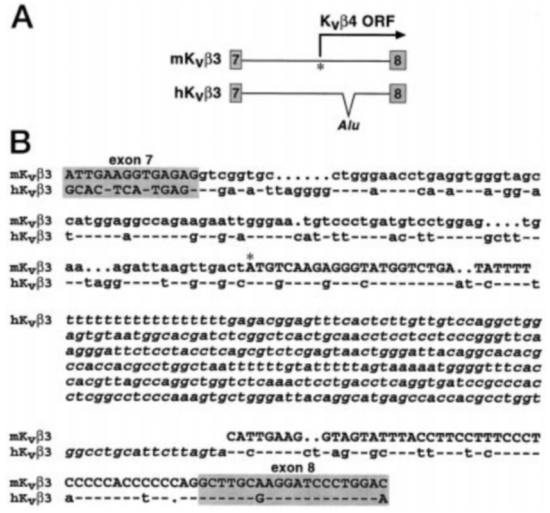

FIG. 6. **Start of ORF of mouse Kvβ4-cDNA (8) in Kvβ3 intron 7.** *A*, schematic diagram showing exons 7 and 8 (*shaded rectangles*) of mouse (*m*) and human (*h*) Kvβ3 genes and intervening sequence (*thin line*) with inserted *Alu* repeat (*Alu*) in hKvβ3. The start site of mouse Kvβ4 ORF is indicated by an *asterisk*. *B*, alignment of mouse (*m*) and human (*h*) Kvβ3 genomic DNA sequences. ORF sequences are in *capital letters*, intron sequences in *lowercase letters*. Exon 7 and 8 sequences are *shaded*. An *asterisk* marks the first ATG of the mouse Kvβ4 ORF (14). Identical nucleotides are indicated by *dashes*. *Dots* indicate gaps introduced for optimal sequence alignment. *Alu* repeat sequence is in *italic letters*.

previously published data for Kv1.5 channels coexpressed with an N(Kvβ3)-C(Kvβ2) chimeric subunit in *Xenopus* oocytes (26). These findings indicate comparable mechanisms for the Kvβ3.1 ball-mediated N-type inactivation observed in the CHO cell and the *Xenopus* oocyte expression system. The opposing results obtained for Kv1.4Δ1–110 (17) and Kv1.5 (26) suggest an intracellular environment in the *Xenopus* oocyte nonpermissive for the functional interaction between Kvβ3.1 and Kv1.5.

The binding of Kvβ1 and Kvβ2 subunits is highly specific for members of the Kv1-subfamily (9, 10). This is consistent with immunoprecipitation experiments of Shamotienko *et al.* (48), who investigated the subunit composition of native Kv channels containing Kvα subunits of the Shaker-related family. Interestingly, mKvβ4, the splice variant of the Kvβ3 gene in mice, can be coimmunoprecipitated with both Kv1.5 and Kv2.2 subunits when coexpressed in Sf9 cells (14). However, coexpression with Kvβ3.1 in CHO cells does not confer rapid inactivation to Kv2.2 channels.[3] Therefore, future experiments should be focused on the question of which Kvα subunits are associated with Kvβ3.1 in native Kv channels.

Acknowledgments—We thank K. Forsman-Semb and O. Sandgren for providing DNA samples from CORD5 families, M. Schwarz and R. Waldschütz for comments on the manuscript, and D. Clausen for graphical assistance.

REFERENCES

1. Hille, B. (1992) *Ionic Channels of Excitable Membranes*, 2nd Ed., Sinauer Associates Inc., Sunderland, MA
2. Chandy, K. G., and Gutman, G. A. (1995) in *Handbook of Receptors and Channels,* Vol. 2, pp. 1–72, CRC Press, Inc., Boca Raton, FL
3. Pongs, O. (1992) *Physiol. Rev.* **72,** S69–S88
4. Pongs, O. (1995) *Neuroscience* **7,** 137–146
5. Jan, L. Y., and Jan, Y. N. (1997) *Annu. Rev. Neurosci.* **20,** 91–123
6. Christie, M. J., North, R. A., Osborne, P. B., Douglass, J., and Adelman, J. P. (1990) *Neuron* **2,** 405–411
7. Isacoff, E. Y., Jan, Y. N., and Jan, L. Y. (1990) *Nature* **345,** 530–534
8. Ruppersberg, J. P., Schröter, K. H., Sakmann, B., Stocker, M., Sewing, S., and Pongs, O. (1990) *Nature* **345,** 535–537
9. Yu, W., Xu, J., and Li, M. (1996) *Neuron* **16,** 441–453
10. Sewing, S., Roeper, J., and Pongs, O. (1996) *Neuron* **16,** 455–463
11. Parcej, D. N., Scott, V. E. S., and Dolly, J. O. (1992) *Biochemistry* **31,** 11084–11088
12. Chouinard, S. W., Wilson, G. F., Schlimgen, A. K., and Ganetzky, B. (1995) *Proc. Natl. Acad. Sci. U. S. A.* **92,** 6763–6767
13. Wilson, G. F., Weng, Z., Chouinard, S. W., Griffith, L. C., and Ganetzky, B. (1998) *J. Biol. Chem.* **273,** 6389–6394
14. Fink, M., Duprat, F., Lesage, F., Heurteaux, C., Romey, G., Barhanin, J., and Lazdunski, M. (1996) *J. Biol. Chem.* **271,** 26341–26348
15. Shi, G., Nakahira, K., Hammond, S., Rhodes, F. R., Schechter, L. E., and Trimmer, J. S. (1996) *Neuron* **16,** 843–852
16. Rettig, J., Heinemann, S. H., Wunder, F., Lorra, C., Parcej, D. N., Dolly, J. O., and Pongs, O. (1994) *Nature* **369,** 289–294
17. Heinemann, S. H., Rettig, J., Wunder, F., and Pongs, O. (1995) *FEBS Lett.* **377,** 383–389
18. England, S. K., Uebele, V. N., Kodali, J., Bennett, P. B., and Tamkun, M. M. (1995) *J. Biol. Chem.* **270,** 28531–28534
19. England, S. K., Uebele, V. N., Shear, H., Kodali, J., Bennett, P. B., and Tamkun, M. M. (1995) *Proc. Natl. Acad. Sci. U. S. A.* **92,** 6309–6313
20. Majumder, K., de Biasi, M., Wang, Z., and Wible, B. A. (1995) *FEBS Lett.* **361,** 13–16
21. McCormack, K., McCormack, T., Tanouye, M., Rudy, B., and Stühmer, W. (1995) *FEBS Lett.* **370,** 32–36
22. Morales, M. J., Castellino, R. C., Crews, A. L., Rasmusson, R. L., and Strauss, H. C. (1995) *J. Biol. Chem.* **270,** 6272–6277
23. Leicher, T., Roeper, J., Weber, K., Wang, X., and Pongs, O. (1996) *Neuropharmacology* **35,** 787–795
24. Uebele, V. N., England, S. K., Chaudhary, A., Tamkun, M. M., and Snyders, D. J. (1995) *J. Biol. Chem.* **271,** 2406–2412
25. de Biasi, M., Wang, Z., Accili, E., Wible, B., and Fedida, D. (1997) *Am. J. Physiol.* **272,** H2932–H2941
26. Heinemann S. H., Rettig J., Graack H. R., and Pongs O. (1996) *J. Physiol.* **493,** 625–633
27. Zagotta, W. N., Hoshi, T., and Aldrich, R. W. (1990) *Science* **250,** 568–570
28. Isacoff, E. Y., Jan, Y. N., and Jan, L. Y. (1991) *Nature* **353,** 86–90
29. Feinberg, A. P., and Vogelstein, B. (1983) *Anal. Biochem.* **132,** 6–13
30. Sanger, F., Nicklen, S., and Coulson, A. R. (1977) *Proc. Natl. Acad. Sci. U. S. A.* **74,** 5463–5467
31. Leicher, T. (1998) *Charakterisierung von β-Untereinheiten humaner Kaliumkanäle*, Ph.D. thesis, Hamburg University
32. Roeper J., Lorra C., and Pongs O. (1997) *J. Neurosci.* **17,** 3379–3391
33. Shapiro, M. B., and Senapathy, P. (1987) *Nucleic Acids Res.* **15,** 7155–7174
34. Weissenbach, J., Gyapay, G., Dib, C., Vignal, A., Morissette, J., Millasseau, P., Vaysseix, G., and Lathrop, M. (1992) *Nature* **359,** 794–801
35. Stathakis, D. G., Hoover, K. B., You, Z., and Bryant, P. J. (1997) *Genomics* **44,** 71–82
36. Oliveira, L., Miniou, P., Viegas-Pequignot, E., Rozet, J. M., Dollfus, H., and Pittler, S. J. (1994) *Genomics* **22,** 478–481
37. Perrault, I., Rozet, J. M., Calvas, P., Gerber, S., Camuzat, A., Dollfus, H., Chatelin, S., Souied, E., Ghazi, I., Leowski, C., Bonnemaison, M., Le Paslier, D., Frezal, J., Dufier, J. L., Pittler, S., Munnich, A., and Kaplan, J. (1996) *Nat. Genet.* **14,** 461–464
38. Kelsell, R. E., Gregory-Evans, K., Payne, A. M., Perrault, I., Kaplan, J., Yang, R. B., Garbers, D. L., Bird, A. C., Moore, A. T., and Hunt, D. M. (1998) *Hum. Mol. Genet.* **7,** 1179–1184
39. Balciuniene, K., Johansson, O., Sandgren, L., Wachtmeister, G., Holmgren, D., and Forsman K. (1995) *Genomics* **30,** 281–286
40. Snyders, D. J., Tamkun, M. M., and Bennett, P. B. (1993) *J. Gen. Physiol.* **101,** 513–543
41. Accili, E. A., Kiehn, J., Yang, Q., Wang, Z., Brown, A. M., and Wible, B. A. (1997) *J. Biol. Chem.* **272,** 25824–25831
42. Roeper, J., Sewing, S., Zhang, Y., Sommer, T., Wanner, S. G., and Pongs, O. (1998) *Nature* **391,** 390–393
43. Schultz, D., Litt, M., Smith, L., Thayer, M., and McCormack, K. (1996) *Genomics* **31,** 389–391
44. Klocke, R., Roberts, S. L., Tamkun, M. M., Gronemeier, M., Augustin, A., Albrecht, B., Pongs, O., and Jockusch, H. (1993) *Genomics* **18,** 568–574
45. Lock, L. F., Debra, J. G., Street, V. A., Migeon, M. B., Jenkins, N. A., Copeland, N. G., and Tempel, B. L. (1994) *Genomics* **20,** 354–362
46. Rhodes, K. J., Monaghan, M. M., Barrezueta, N. X., Nawoschik, S., Bekele-Arcuri, Z., Matos, M. F., Nakahira, K., Schechter, L. E., and Trimmer, J. S. (1996) *J. Neurosci.* **16,** 4846–4860
47. Morales, M. J., Wee, J. O., Strauss, H. C., and Rasmusson, R. L. (1995) *Proc. Natl. Acad. Sci. U. S. A.* **93,** 15119–15123
48. Shamotienko, O. G., Parcej, D. N., and Dolly, J. O. (1997) *Biochemistry* **8,** 8195–8201
49. Kelsell, R. E., Evans, K., Gregory, C-Y., Moore, A. T., Bird, A. C., and Hunt, D. M. (1997) *Hum. Mol. Genet.* **6,** 597–600

[3] R. Bähring, unpublished observation.